

## Relationship between Solid-State $^{31}\text{P}$ NMR Parameters and X-ray Structural Data in Some Zinc Phosphonates

Dominique Massiot,<sup>†</sup> Stéphanie Drumel,<sup>‡</sup>  
Pascal Janvier,<sup>§</sup> Martine Bujoli-Doeuff,<sup>‡</sup> and  
Bruno Bujoli<sup>\*,§</sup>

Centre de Recherches sur la Physique des Hautes  
Températures, UPR CNRS 4212  
1D Avenue de la Recherche Scientifique  
45071 Orléans Cedex 02, France  
Institut des Matériaux de Nantes  
UMR CNRS 0110, 2 Rue de la Houssinière  
44072 Nantes Cedex 03, France  
Laboratoire de Synthèse Organique  
URA CNRS 475, 2 Rue de la Houssinière  
44072 Nantes Cedex 03, France

Received August 5, 1996

Revised Manuscript Received October 16, 1996

Metal phosphonate chemistry is attracting increasing interest because of the variety of properties than can be introduced via the phosphonate ligand.<sup>1</sup> These hybrid materials contain a  $\text{PO}_3$ /metal inorganic core, separated by the organic moiety bound to phosphorus.

In our group, we conceived the idea of preparing covalently immobilized catalysts (manganese porphyrins, bipyridine rhodium complexes, etc.) simply by a functionalization of the desired catalytic complexes with phosphonic acid units, followed by the polymerization of the phosphonate network around these complexes, according to an encapsulation concept.<sup>2</sup> However, to have a better understanding of the catalytic activity of the resulting supported catalysts, structural information is required regarding the environment of the catalytic site as well as the porosity of the material that is related to the nature of the inorganic framework. The main problem generally lies in the amorphous nature of this type of compound and even X-ray powder structure determinations, which have proved to be helpful in the case of polycrystalline phosphonates,<sup>3</sup> cannot be used in this case.

As the main part of our catalytic complexes were immobilized as diamagnetic zinc phosphonates, we wanted to know if solid-state  $^{31}\text{P}$  NMR spectroscopy could be used as an investigation tool to provide structural information about the environment of the phosphorus atoms. We can note that solid-state NMR spectroscopy has already been used to characterize phosphonic acids<sup>4</sup> ( $^{31}\text{P}$  CP-MAS) and zirconium carboxy-

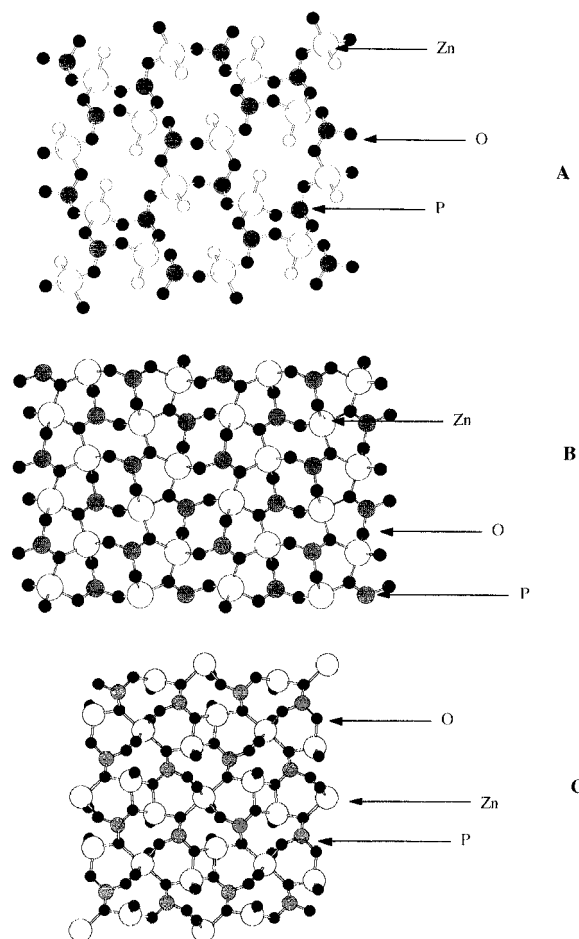


**Figure 1.** Examples of in-plane structure of layered zinc phosphonates showing (A) a (111) connectivity for the  $\text{PO}_3$  groups  $[\text{Zn}(\text{O}_3\text{PC}_2\text{H}_4\text{NH}_2)]$ , (B) a (112) connectivity  $[\text{Zn}_3(\text{O}_3\text{PC}_2\text{H}_4\text{CO}_2)_2 \cdot 3\text{H}_2\text{O}]$ , (C) a (122) connectivity  $[\text{Zn}_3(\text{O}_3\text{PC}_2\text{H}_4\text{CO}_2)_2]$ .

alkylphosphonates<sup>5</sup>  $\text{Zr}(\text{O}_3\text{PCH}_2\text{CO}_2\text{H})_2$  ( $^{31}\text{P}$  and  $^{13}\text{C}$  CP-MAS, to get structural details of the organic pendant groups present in the interlayer space).

In previous studies, we have prepared many crystallized zinc phosphonates, the structure of which have been determined, thus allowing us to use these compounds as references. From these structural data, we have noticed that the  $\text{PO}_3$  groups, when no proton was retained on the oxygen atoms, could be coordinated in three different ways: (i) either each of the three oxygen atoms of the phosphonate unit is coordinated to only one zinc atom (Figure 1A) and the connectivity is noted (111); (ii) in the second case, one of these oxygens is bridging two zinc atoms, while the two others are bonded only to one metal atom and the connectivity is (112) (Figure 1B); (iii) in the last case, two bridging oxygens are now present with a (122) connectivity (Figure 1C). We have recorded the solid-state  $^{31}\text{P}$  NMR spectra of our series of reference samples at different spinning rates, in order to know if these different connectivities could be differentiated using this technique.  $^1\text{H}$ -to- $^{31}\text{P}$  cross polarization and  $^1\text{H}$  decoupling (50 kHz field strength, 5 s recycle delay, 16–64 transients, DSX 300 Bruker spectrometer) were used in all cases, with both magic angle spinning (MAS, 2–6 kHz) and static conditions. The isotropic chemical shifts were extracted from the high-speed MAS spectra, which

<sup>†</sup> UPR CNRS 4212.

<sup>‡</sup> UMR CNRS 0110.

<sup>§</sup> URA CNRS 475.

(1) See for example: Clearfield, A. *New Developments in Ion Exchange Materials*; Kodansha, Ltd.: Tokyo, 1991. Wan, B. Z.; Anthony, R. G.; Peng, G. Z.; Clearfield, A. *J. Catal.* **1994**, *101*, 19–27. Cao, G.; Hong, H.; Mallouk, T. E. *Acc. Chem. Res.* **1992**, *25*, 420–427. Katz, H. E. *Chem. Mater.* **1994**, *6*, 2227–2232. Thompson, M. E. *Chem. Mater.* **1994**, *6*, 1168–1175.

(2) Deniaud, D.; Schöllhorn, B.; Mansuy, D.; Rouxel, J.; Battioni, P.; Bujoli, B. *Chem. Mater.* **1995**, *7*, 995–1000.

(3) Poojary, D. M.; Grohol, D.; Clearfield, A. *Angew. Chem., Int. Ed. Engl.* **1995**, *34*, 1508–1510. Poojary, D. M.; Clearfield, A. *J. Am. Chem. Soc.* **1995**, *117*, 11278–11284.

(4) Harris, R. K.; Merwin, L. H.; Hägele, G. *Magn. Reson. Chem.* **1989**, *27*, 470–475.

(5) Burwell, D. A.; Valentine, K. G.; Timmermans, J. H.; Thompson, M. E. *J. Am. Chem. Soc.* **1992**, *114*, 4144–4150.

**Table 1.**  $^{31}\text{P}$  Chemical Shift Tensor Data for a Series of Zinc Phosphonates

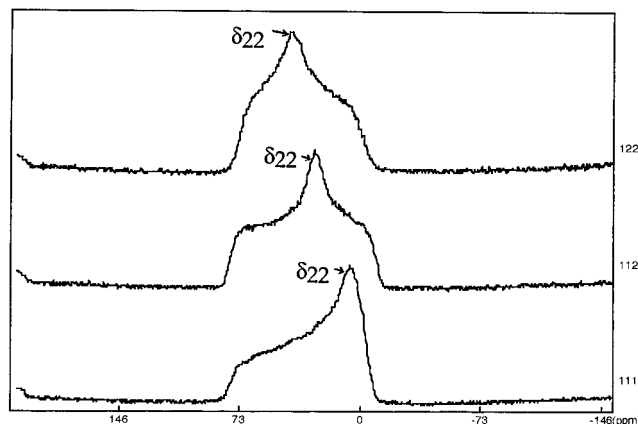
compound	ref	connectivity	$\delta_{\text{iso}}^a$ (ppm)	$\eta^b$	$\Delta^c$	$\delta_{11}$ (ppm)	$\delta_{22}$ (ppm)	$\delta_{33}$ (ppm)	$\eta_e^d$
$\text{Zn}(\text{O}_3\text{PC}_2\text{H}_4\text{NH}_2)$	7	(111)	27.0	0.4	50.5	-7.1	10.6	77.5	0.4
$\text{Zn}(\text{O}_3\text{PC}_2\text{H}_4\text{CO}_2\text{H}) \cdot \frac{1}{2}\text{C}_6\text{H}_5\text{NH}_2$ (site 1 (50%))	8	(111)	28.9	0.4	43.1	-1.3	16.0	72.0	0.4
$\text{Zn}(\text{O}_3\text{PC}_2\text{H}_4\text{CO}_2\text{H}) \cdot \frac{3}{2}\text{H}_2\text{O}$	9	(111)	29.8	0.4	46.8	-3.0	15.8	76.6	0.4
$\text{Zn}_3(\text{O}_3\text{PC}_2\text{H}_4\text{CO}_2)_2 \cdot 3\text{H}_2\text{O}$	9,10	(112)	32.4	0.8	46.9	-9.8	27.7	79.3	0.8
$\text{Zn}(\text{O}_3\text{PC}_2\text{H}_4\text{CO}_2\text{H}) \cdot \frac{1}{2}\text{C}_6\text{H}_5\text{NH}_2$ (site 2 (50%))	8	(112)	34.4	0.8	43.1	-4.4	30.1	77.5	0.8
$\text{Zn}_3(\text{O}_3\text{PC}_2\text{H}_4\text{CO}_2)_2$	9	(122)	35.9	0.9	-33.8	68.0	37.6	2.1	1.1
$\text{Zn}(\text{O}_3\text{PC}_2\text{H}_4\text{CO}_2\text{H}) \cdot \text{H}_2\text{O}^e$	9	(122)	38.1	0.9	-38.2	73.5	41.0	-0.1	1.1
$\text{Zn}(\text{O}_3\text{PC}_2\text{H}_5) \cdot \text{H}_2\text{O}^e$	9	(122)	37.7	0.9	-35.8	71.7	39.5	1.9	1.1

<sup>a</sup> All values are given with respect to the isotropic chemical shift constant for 85%  $\text{H}_3\text{PO}_4$ . <sup>b</sup> Chemical shift asymmetry defined as  $|\delta_{22} - \delta_{11}|/|\delta_{33} - \delta_{\text{iso}}|$  with the Haeberlen convention.<sup>11</sup> <sup>c</sup> Chemical shift anisotropy defined as  $\delta_{33} - \delta_{\text{iso}}$ . <sup>d</sup> Extended value of  $\eta$  defined as  $\eta_e = \eta$  ( $\Delta > 0$ );  $\eta_e = 2 - \eta$  ( $\Delta < 0$ ). <sup>e</sup> Same in-plane structure, simply differing by the nature of the organic chain bound to phosphorus.

consisted of a center band which was a single narrow line (half-height line width 70 Hz), except for  $\text{Zn}(\text{O}_3\text{PC}_2\text{H}_4\text{CO}_2\text{H}) \cdot \frac{1}{2}\text{C}_6\text{H}_5\text{NH}_2$ , where two sites [(111) 50%, (112) 50%] are present. The principal components of the chemical shift tensors were measured using the spinning sidebands fitting routine,<sup>6</sup> and a recapitulative list of the values that led to the best fits for the different observation conditions (static and MAS at different spinning rate) is given in Table 1.

We can first notice that the isotropic chemical shifts  $\delta_{\text{iso}}$  move downfield as the connectivity increases, corresponding to an increase in the paramagnetic contribution to the nuclear shielding, as the number of zinc atoms connected to the  $\text{PO}_3$  groups varies from 3 to 5. A similar behavior was recently reported by Aime et al. in tricadmium phosphates.<sup>12</sup> If we look now at the variation of the chemical shift asymmetry, a  $\delta_{22}$  value close to that of  $\delta_{11}$  is observed in the case of a (111) connectivity, where a pseudoaxial symmetry is present. Then, as the connectivity gets higher to (112) and (122)  $\delta_{22}$  moves from the right side to the left side of the static band, respectively (Figure 2), with a change in the sign of the chemical shift anisotropy (in the case of a (122) site). This discontinuity in the sign of the tensor axiality  $\Delta$  arises from the sorting protocol of the  $\delta_{xx}$  values established by Haeberlen<sup>11</sup> (where  $\delta_{33}$  has the maximum absolute distance to  $\delta_{\text{iso}}$ ) and might be misleading. A better representation of the evolution of the  $^{31}\text{P}$  NMR spectra with the connectivity is given by the  $\eta$  parameter, made continuous defining  $\eta_e$  (extended chemical shift asymmetry), ranging from 0 to 2 and calculated as indicated in Table 1.

These preliminary results clearly show that on the basis of the  $\eta_e$  value, it is possible to differentiate (111) [ $\eta_e = 0.4$ ], (112) [ $\eta_e = 0.8$ ], and (122) [ $\eta_e = 1.1$ ] connectivities of the  $\text{PO}_3$  groups in our series of zinc phosphonates. Thus, this simple method gives a satisfactory correlation between the  $^{31}\text{P}$  chemical shift and

**Figure 2.** Characteristic  $^{31}\text{P}$  static spectra of the three types of connectivity present in zinc phosphonates.

the crystallographic sites of  $\text{RPO}_3$  groups in various zinc phosphonates structures. To apply this method for the determination of  $\text{PO}_3$  environments in zinc phosphonates of unknown structure, additional data, using structurally characterized zinc phosphonates present in the literature, are actually collected to complete our series of reference compounds. To strengthen the validity of this method, measurements were carried out on two zinc phosphonates for which X-ray data were not available:  $\text{Zn}(\text{O}_3\text{PCH}_3)$  and  $\text{Zn}(\text{O}_3\text{PCH}_3) \cdot n\text{-C}_4\text{H}_9\text{NH}_2$ . From a XANES-EXAFS study,<sup>8</sup> we had previously assumed that a (112) connectivity was present for the former compound, while the latter compound corresponded to a (111) environment for the  $\text{PO}_3$  groups. The  $^{31}\text{P}$  MAS NMR results are in very good agreement with this hypothesis: a  $\eta_e$  value of 0.8 for  $\text{Zn}(\text{O}_3\text{PCH}_3)$  [ $\delta_{\text{iso}} = 32.6$ ;  $\delta_{11} = -5.1$ ;  $\delta_{22} = 28.4$ ;  $\delta_{33} = 74.4$ ;  $\Delta = 41.8$  ppm] and a  $\eta_e$  value of 0.4 for  $\text{Zn}(\text{O}_3\text{PCH}_3) \cdot n\text{-C}_4\text{H}_9\text{NH}_2$  [ $\delta_{\text{iso}} = 27.7$ ;  $\delta_{11} = -8.0$ ;  $\delta_{22} = 11.7$ ;  $\delta_{33} = 79.4$ ;  $\Delta = 51.7$  ppm]. The influence of the metal associated to the  $\text{PO}_3$  groups (i.e., Zr(IV), Al(III), Ga(III), Bi(III), Cd(II), etc.) are also under investigation, in order to estimate the possible extension of the method to other metal phosphonates. For example, in the case of  $\text{Zr}(\text{O}_3\text{PC}_2\text{H}_5)_2$ , a structural analogue of  $\alpha\text{-ZrP}$  in which a (111) connectivity is present,<sup>13</sup> a  $\eta_e$  value of 0.4 was found [ $\delta_{\text{iso}} = 7.8$ ;  $\delta_{11} = -8.4$ ;  $\delta_{22} = 1.6$ ;  $\delta_{33} = 30.3$ ;  $\Delta = 22.5$  ppm], consistent with the observations made in the zinc phosphonates series. In conclusion, this method would be the ideal complement of Zn K-edge EXAFS spectroscopy, to get structural informations about both metal and phosphorus environments.

CM960417X

(6) Massiot, D.; Thiele, H.; Germanus, A. *Bruker Rep.* **1994**, 140, 1762. Herzfeld, J.; Berger, A. E. *J. Chem. Phys.* **1980**, 73, 6021.

(7) Drumel, S.; Janvier, P.; Deniaud, D.; Bujoli, B. *J. Chem. Soc., Chem. Commun.* **1995**, 1051-1052.

(8) Drumel, S.; Janvier, P.; Bujoli-Doeuff, M.; Bujoli, B. *J. Mater. Chem.* **1996**, 6, 1843-1847.

(9) Drumel, S.; Janvier, P.; Barboux, P.; Bujoli-Doeuff, M.; Bujoli, B. *Inorg. Chem.* **1995**, 34, 148-156.

(10) Cao, G.; Rabenberg, L. K.; Nunn, C. M.; Mallouk, T. E. *Chem. Mater.* **1991**, 3, 149-156.

(11) Haeberlen, U. *High Resolution NMR in Solids: Selective Averaging*. In *Advances in Magnetic Resonance*; Academic Press: New York, London, 1976; Suppl. 1, p 9.

(12) Aime, S.; Digilio, G.; Gobetto, R.; Bigi, A.; Ripamonti, A.; Roveri, N.; Gazzano, M. *Inorg. Chem.* **1996**, 35, 149-154.

(13) Dines, M. B.; DiGiacomo, P. M. *Inorg. Chem.* **1981**, 20, 92-97.